POSSIBLE FORMATION MECHANISMS OF CHROMITE AND MELT INCLUSION TRAILS IN YAMATO 980459 SHERGOTTITE OLIVINE: IMPLICATIONS FOR ITS THERMAL HISTORY.

S. Che[1], A. J. Brearley[1], and C. K. Shearer[1,2], [1]Department of Earth and Planetary Sciences, 1University of New Mexico, Albuquerque, NM 87131, USA (shaofanche@unm.edu; brearley@unm.edu), [2]Institute of Meteoritics, 1University of New Mexico, Albuquerque, NM 87131, USA (cshearer@unm.edu).

Introduction: Martian shergottites display a large range of oxygen fugacities (fO_2) (up to 4 log units), which are partially correlated with the incompatible-element features (e.g., La/Yb, $^{87}Sr/^{86}Sr$ and $^{143}Nd/^{144}Nd$ ratios) [e.g., 1, 2]. This correlation has been interpreted as evidence that shergottites are derived from two distinct reservoirs: reduced, incompatible-element-depleted and oxidized, incompatible-element-enriched. Two end-member models have been proposed to explain this feature: the crustal assimilation model [e.g., 1] and the heterogeneous mantle model [e.g., 3]. Melt characteristics preserved in olivine in shergottites have been used to examine both of these models. The fO_2 history of Martian magmas has been reconstructed using both Cr (and V) redox state in olivine and oxide-silicate equilibria (e.g., olivine-chromite-orthopyroxene) [1,2,4,5]. Measurements of H and D/H in melt inclusions trapped in olivine have been used to identify the volatile element characteristics of Martian basalt source regions, and the Martian crust [6]. These observations have been extended to define the interactions between these two volatile reservoirs [6]. Therefore, it is critical to fully understand the nature of these magmatic fingerprints preserved in olivine.

In this study, we present detailed high-resolution back-scattered electron (BSE) images of chromite and melt inclusions in olivine phenocrysts from Yamato 980459 (Y-98), a sample believed to represent a primitive Martian melt. We focus on the linear arrays of chromite and melt inclusion trails, which have not been reported previously in shergottites, and discuss their possible formation mechanisms and implications for the sample's thermal history.

Methodology: High-resolution BSE images and X-ray maps were obtained using a FEI Quanta 3D FEG-SEM/FIB instrument fitted with an EDAX Apollo 40 SDD Energy Dispersive Spectroscopy (EDS) system.

Results: Four different types of Cr-rich inclusions are found in Y-98 olivine phenocrysts: (1) Cr-rich inclusion trails with some of the chromite grains associated with glass or orthopyroxene (type I); (2) isolated, euhedral chromite grains commonly associated with glass and/or orthopyroxene (type II); (3) symplectic intergrowths of chromite and orthopyroxene (type III); (4) relatively coarse-grained chromite with orthopyroxene ± glass rims (type IV).
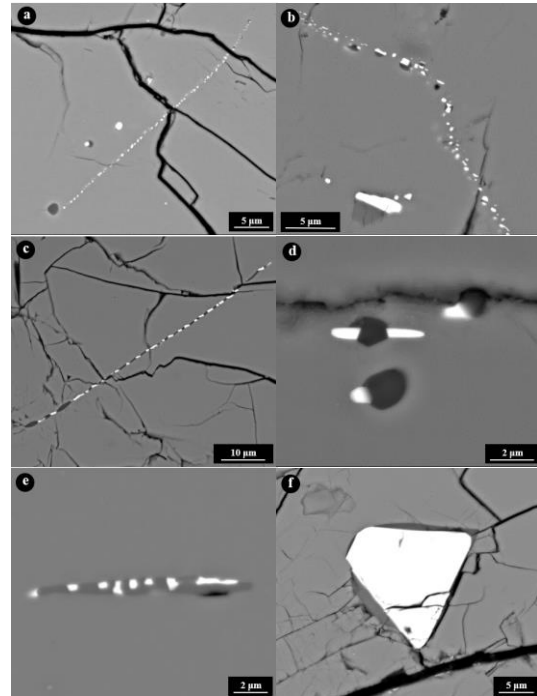

Fig 1. Different types of Cr-rich inclusions: (a-c) type I; (d) type II; (e) type III; (f) type IV.

Type I inclusions are commonly observed in our sample. This type of inclusion is present in many megacrysts, but is absent in others. They are composed of euhedral-to-subhedral Cr-rich gains (<1μm in diameter), some of which coexist with glass or orthopyroxene (Fig. 1a). The compositions obtained using EDS are consistent with chromite plus a subordinate amount of spinel component in solid solution. Most of the trails are single arrays, though two or multiple arrays are also common. The elongation directions of chromite are parallel or subparallel to the trail. Careful examination of the inclusions reveals that some of them are texturally similar to type II and IV inclusions. The trails are not always straight, but often curved or even kinked (Fig. 1b). Preliminary X-ray mapping shows that the trails are not related to Fe-Mg zoning. Chromite grains are interconnected by glass in some cases, with the glass displaying oval shapes (Fig. 1c).

Chromite grains associated with glass in type II inclusions (1-10μm) usually have elongated shapes (Fig. 1d). Chromite enclosed in orthopyroxene has a more complex shape, and some of these inclusions are similar to type III inclusions. Those orthopyroxene grains

show euhedral-to-subhedral shapes. Glass is also present, sometimes in chromite+orthopyroxene inclusions.

Type III inclusions (>5μm in length; Fig. 1e) are commonly observed in extraterrestrial samples [e.g., 5, 7]. We do not focus on this type of inclusion, but we note that type II and III inclusions might be related due to their similarity in texture.

Type IV inclusions (≈10μm; Fig. 1f) have been previously described by [2] in the lherzolitic shergottite ALH 77005, and the rims were interpreted as products of reaction between chromite and trapped melt. Chromites in these inclusions are typically larger than 10μm in diameter, and have euhedral-to-subhedral shapes.

Discussion: Below we discuss three possible mechanisms for the origin of type I inclusions and the implications for each mechanism for interpreting the record preserved in the olivine: (1) exsolution from the host olivine; (2) precipitation along growth surfaces; (3) crystallization from trapped melts along cracks.

Exsolution of Cr-rich symplectites in olivine has been extensively studied in various terrestrial and extraterrestrial samples, and there is a general agreement on their formation mechanism: diffusion of Cr^{3+} from the olivine structure due to lattice contraction during cooling and the subsequent nucleation and growth of chromite as a precipitate [e.g., 7]. This diffusion mechanism could potentially explain some of the inclusion trails; however, the chromites in the inclusion trails do not show symplectic textures. Another argument against the exsolution mechanism is that the presence of significant Cr^{3+} in olivine required to account for the ubiquitous type I inclusions seems to be contrary to the measured Cr^{2+}/Cr^{total} values of olivine [8]. We would expect to see more abundant inclusions on the periphery of olivine, where Cr^{2+}/Cr^{total} values decrease due to a late-stage oxidation event [e.g. 9], if the inclusion trails are the result of exsolution. Recently, [4] used chromium micro X-ray absorption near edge spectroscopy (Cr-μXANES) to estimate fO_2 of the parental magma of Y-98. A potential obstacle to applying this method to shergottites is the presence of tiny Cr-rich inclusions in olivine. For example, if these grains formed by exsolution, they may record changes in the redox conditions during cooling, and thereby modifying the estimated fO_2 values recorded in the olivine. However, more work is needed to unambiguously rule out the exsolution mechanism for these inclusions.

Oscillatory zoning of several incompatible and slow-diffusing elements (e.g., P and Al) is commonly observed in olivine from both natural and experimental samples [e.g., 9]. Boundary layer enrichments and solute trapping are the two proposed mechanisms [9] for this zoning. Concentrations of Cr and P are often positively correlated due to a coupled substitution. It is thus plausible that chromite precipitated from high-Cr zones parallel to the olivine growth surfaces. In this case, the Cr-rich trails record changing growth rates during olivine crystallization, and the associated pyroxene and glass represent trapped melts. Recent studies [e.g., 10, 11] used melt inclusions to reveal compositional variations of shergottite parental magmas. An early incorporation of an oxidized component in depleted shergottites has important implications for their thermal histories, and this might be better constrained by studying inclusion trails, assuming that they are related to olivine growth patterns.

An alternative explanation for the inclusion trails is that they represent trapped melts along cracks. Melt and fluid inclusion trails are common features in terrestrial mantle xenoliths. Late-stage melts can infiltrate into olivine along cracks, crystallizing secondary phases [e.g., 12]. In fact, olivine cores in Y-98 have been interpreted to have a xenocrystic origin [e.g., 9]; thus, a similar origin might apply to our sample. Alternatively, the trails are interstitial melts trapped in fractures at early stages [e.g., 13]. In either case, the fractures healed later, leaving no traces in olivine. The presence of chromite interconnected by glass (Fig. 1c) seems to be consistent with this mechanism.

Further work: At present, we cannot fully distinguish between the above mechanisms for the formation of the chromites in the olivine megacrysts. To help differentiate between these different possibilities we will prepare focused-ion-beam (FIB) sections to investigate the microstructural characteristics of chromite and its associated phases using transmission electron microscopy (TEM). This work will establish the possible crystallographic relationships with the host olivine, which are indicative of exsolution processes. Analytical TEM will be used to determine the compositions of the chromites to compare to those of primary magmatic, coarse-grained chromites.

References: [1] Herd C. D. et al. (2002) *GCA, 66(11)*, 2025-2036. [2] Goodrich C. A. et al. (2003) *MAPS, 38(12)*, 1773-1792. [3] Borg L. E. et al. (2003) *GCA, 67(18)*, 3519-3536. [4] Bell A. S. et al. (2014) *AM, 99(7)*, 1404-1412. [5] Bell P. M. et al. (1975) *6th LPSC*, 231-248. [6] Usui T. et al. (2015) *EPSL, 410*, 140-151. [7] Goodrich C. A. et al. (2014) *GCA, 135*, 126-169. [8] Bell A. S. et al. (2015) 46th LPSC, #2421. [9] Shearer C. K. et al. (2013) *GCA, 120*, 17-38. [10] Usui T. et al. (2012) *EPSL, 357*, 119-129. [11] Peters T. J. et al. (2015) *EPSL, 418*, 91-102. [12] Golovin A. V. and Sharygin V. V. (2007) *RGG, 48(10)*, pp.811-824. [13] Neumann E. R. and Wulff-Pedersen E. (1997) *JP, 38(11)*, 1513-1539.